

## Polydispersity-linked Memory Effects in a Magnetic Nanoparticle System

S.Chakraverty<sup>1</sup>, A.Frydman<sup>2</sup>, M.Bandyopadhyay<sup>1</sup>, S.Dattagupta<sup>1</sup>, Surajit Sengupta<sup>1</sup> and P.A.Sreeram<sup>1</sup><sup>1</sup> Nanoscience Unit, S.N.Bose National Centre for Basic Sciences,  
Block-JD, Sector-III, Salt Lake, Kolkata - 700098, India.<sup>2</sup> Dept. of Physics, Bar Ilan University, Ramat Gan 52900, Israel

(Dated: April 14, 2024)

We have performed a series of measurements on the low temperature behavior of a magnetic nanoparticle system. Our results show striking memory effects in the dc magnetization. Dipolar interactions among the nano-particles suppress the memory effect. We explain this phenomenon by the superposition of different superparamagnetic relaxation times of single domain magnetic nanoparticles. Moreover, we observe a crossover in the temperature dependence of coercivity. We show that a dilute dispersion of particles with a flat size distribution yields the best memory.

PACS numbers: 75.75.+a, 75.50.Lk, 75.50.Tt, 75.20.-g

Single domain magnetic nano-particles [1, 2, 3, 4, 5, 6, 7, 8] possess relaxation times that depend exponentially on the volume [9, 10, 11, 12]. Thus polydispersity leads to a distribution of relaxation times [13, 14], those larger than the measurement time yielding 'frozen' behavior, and those shorter giving rise to 'magnetic viscosity' [11, 12]. A given sample then displays strong memory effects, which are reported here. Our results are based on the measurements of temperature-dependent magnetization during cooling and heating cycles. These memory effects may have important device applications [3] in the future.

In this Letter we report results on magnetization and coercivity measurements in systems of  $\text{NiFe}_2\text{O}_4$  particles (mean size  $\sim 3\text{nm}$ ) embedded in a  $\text{SiO}_2$  matrix. Both measurements show strong history dependent effects depending on the separation between the particles and hence their mutual interaction. We prepare the samples by using a sol-gel [15] technique. The ratio of  $\text{NiFe}_2\text{O}_4$  to  $\text{SiO}_2$  is 1:1 and 3:7 by weight, for sample A and sample B respectively. The ferrite to matrix ratio is altered in order to tune the interparticle interaction. The phase of the samples is identified by X-ray diffraction [16] using a Philips PW 1710 diffractometer with  $\text{Cu K}$  radiation ( $\lambda = 1.54 \text{ \AA}$ ). The average particle size is estimated by X-ray diffraction as well as by a JEM-200-CX transmission electron micrograph (TEM). DC magnetization measurements are performed on a Quantum Design superconducting interference device magnetometer (MPMS) from 300K to 4K.

The X-ray diffraction spectrum confirms that our sample is indeed in a single-phase of ferrite  $\text{NiFe}_2\text{O}_4$  with no residual  $-\text{Fe}_2\text{O}_3$ . The average particle size of the nanophase  $\text{NiFe}_2\text{O}_4$ , estimated from the broadening of X-ray diffraction peak is  $\sim 3\text{nm}$  for both the samples. The TEM micrograph of the samples suggests that the particles are spherical in shape and the particle size follows a log-normal [14] distribution. The interparticle separation measured from TEM micrographs are  $\sim 5\text{nm}$  for sample A and  $\sim 15\text{nm}$  for sample B.

The magnetization measurements are carried out in ac-

cordance with the following cooling and heating protocol. At  $T = 300\text{K}$  ( $T = T_1$ ), a small magnetic field ( $H = 50 \text{ Oe}$ ) is applied and the magnetization ( $M$ ) measured. Keeping the field on, the temperature ( $T$ ) is lowered continuously at a steady rate to  $T_n$  and  $M$  is simultaneously measured up to temperature  $T_n$ . Thus one obtains  $M$  versus  $T$  in the cooling regime ( $T_n \leq T \leq T_1$ ). At  $T_n$  the field is switched off and the drop of  $M$  is monitored for several ( $\sim 4$ ) hours. Subsequently, the magnetic field is switched back on and  $M(T)$  versus  $T$  is mapped in the cooling regime ( $T_{n-1} \leq T \leq T_n$ ). At  $T_{n-1}$  the field is switched off again and the process of measurement repeated, until the lowest temperature  $T_0$  is reached. Thus, one obtains field-cooled response and zero-field relaxation of the magnetization as a function of temperature. At the end of the cooling cycle, at  $T_0$ , the field is turned on and  $M(T)$  monitored as the system is heated from  $T_0$  through  $T_{n-2}, T_{n-1}, T_n$  and eventually to  $T_1$ , the magnetic field remaining on throughout. Our results are shown in Fig.1, for two distinct values of interparticle spacing  $5\text{nm}$  (sample A), and  $15\text{nm}$  (sample B). The heating path surprisingly shows wiggles in  $M(T)$  at all the  $T$  steps  $T_{n-2}, T_{n-1}, T_n$  where  $H$  was earlier switched off during cooling, apparently retaining a memory of the temperature steps at which the cooling was arrested.

One tantalizing aspect of our results is that memory effects are more prominent for sample B than for sample A, although in the latter the average inter-particle distance is smaller and hence the dipolar interaction larger. Recently Sun et. al. [13] have reported very similar history dependent effects in the magnetization measurements of a monolayer of sputtered perm alloy ( $\text{Ni}_{81}\text{Fe}_{19}$ ) clusters on a  $\text{SiO}_2$  substrate. These authors attribute the disparate cooling and heating histories to aging and concomitant memory effects found in a spin glass phase [17]. Spin glass transitions are known to occur due to disorder and frustration [18] in dilute magnetic alloys that are characterized by a complicated free energy landscape with deep valleys and barriers. Strongly nonequilibrium

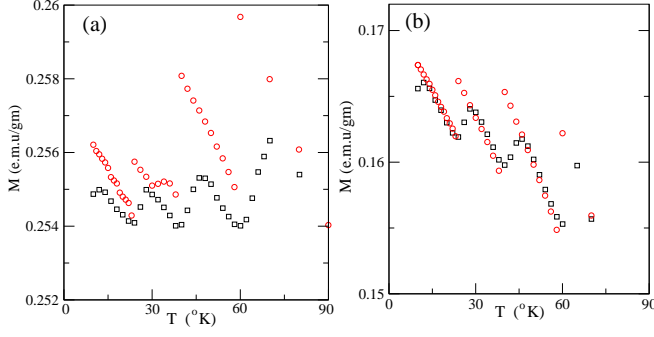


FIG .1: (color on-line) Experimental  $M(T)$  curves during cooling (2 red) in a small magnetic field  $H = 50$  Oe and zero-field heating (3 black) for the (a) interacting and (b) non-interacting samples showing prominent memory effects. A constant heating/cooling rate of 2 K was maintained except at 60, 40 and 20 K where the cooling was arrested for 4 h duration at each temperature during which time  $H$  was switched off.

memory dependent behavior ensues as a result of the system getting trapped in a deep valley [19] such that the relaxation time ( $\tau$ ) for deactivation becomes long compared to experimental time scales of measurement.

Our interpretation of the results shown in Fig.1 is very different from that of [13]. We demonstrate below that the observed phenomena (by us as well as by other groups) are not connected to complicated spin glass type interactions but can be simply attributed to a superposition of relaxation times, arising from particle size distribution, as it were in noninteracting single-domain magnetic particles. Experimentally it is known [14] that nano particle sizes are usually distributed according to a log-normal distribution. However, we show below that the exact form of the distribution is irrelevant for explaining the memory effect. In fact, in order to keep the analysis simple and to obtain a clear understanding of the physics it is sufficient to take a simple size distribution consisting of two delta function peaks so that there are only two kinds of particles "large" (volume  $V_1$ ) and "small" ( $V_2$ ). Correspondingly we have only two relaxation times  $\tau_1$  and  $\tau_2$  in our model, if we remember [9, 10, 11] that:

$$\tau_i / \tau_0 = \exp \left[ \frac{(K V_i - H V_i)}{K_B T} \right]; \quad (1)$$

where  $K$  is the anisotropy energy,  $\tau_0$  is the magnetic moment per unit volume,  $H$  is the applied magnetic field and  $K_B$  is the Boltzmann constant [12]. Our interpretation of the observed results hinges on the premise

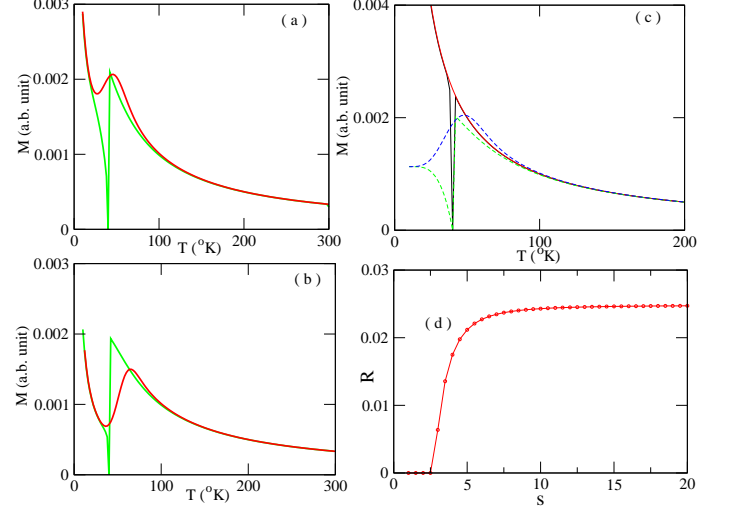


FIG .2: (color on-line) Simulated  $M$  (arbitrary unit) vs.  $T$  curves during cooling and heating for the (a) interacting and (b) non-interacting cases: The curve (c) shows the various contributions to the total magnetization (thick solid line) of interacting sample (A) coming from the fast (thin solid line) and slow (dashed line) particles. The theoretical curves (a) - (c) have been calculated using a double delta function distribution of particle sizes. Curve (d) shows a plot of the recovery parameter  $R$  (see text) as a function of the width ( $s$ ) of a Gaussian particle size distribution.

that the time  $\tau_1$  is much larger than the measurement time while  $\tau_2$  is much smaller, at the lowest measured temperature ( $T_0$ ). Both  $\tau_1$  and  $\tau_2$  are expected to be smaller than the measurement time at the highest temperature  $T_1$ . Therefore, in the intermediate temperature domain ( $T_0 < T < T_1$ ), the small particles equilibrate rapidly, thus showing superparamagnetic viscosity [12] while the large particles are 'blocked'. This is observed in Fig 2 (c) where we have plotted computer simulations [20] of  $M(T)$  separately for the two sets of interacting (separation distance of  $\sim 5$  nm) particles under the same cooling and heating regimens. Here we choose the temperature  $T$  at which  $H$  is switched off such that the blocking temperatures [9, 10] corresponding to the two different particle sizes rank  $T$ . The simulations are based on standard rate theory calculation for the time dependent magnetization [20]. When  $H$  is zero, both sets of particles relax to  $M = 0$ . However, when  $H$  is turned on, particles 1 are blocked ( $M = 0$ ) while 2 show facile response. As  $T$  is increased again,  $M$  for particles 2 decreases with  $T$  while  $M$  for particles 1 initially increases before dropping off. The resultant graph is a superposition (see Fig 2 (c)) of a monotonically decreasing curve and a hump, thus producing a wiggle. This effect is seen only when the temperature of arrest is in-between the two respective blocking temperatures, in conformity with the

ndings of [14].

We have performed measurements on the same system but now with increased interparticle separation ( $\sim 15\text{nm}$ ) (see Fig.1(b)), the simulation results of which are shown in Fig.2(b).

The resultant interaction effect due to dipole-dipole coupling, not considered in [14], is also quite distinct from the quenched-in disorder mediated interactions proposed in [13]. Since the dipole moment of a single-domain particle is proportional to its volume, the effect of interaction, within a mean-field picture, may be incorporated by adding a term proportional to  $V^2$  in the exponent of  $\langle V \rangle$ . Thus, even small particles ( $V_2$ ) can now have  $\tau_2$  larger than the measurement time. This becomes more prominent at lower temperatures. Therefore, the blocking temperatures for both particles 1 and 2 are now shifted to higher  $T$ , thereby causing the wiggles to disappear. This is consistent with the results of Fig.1 which show that the memory effects are stronger for the non-interacting particles. We conclude then that the unexpected wiggles seen in the cooling and heating cycles of  $M(T)$  versus  $T$  have much less to do with interaction effects but more to do with polydispersity of the sample. How crucially does the nature of the particle size distribution affect the magnetization recovery during the zero-field heating cycle? In order to answer this question we first quantify the memory effect by defining a parameter,

$$R = \left( \frac{dM}{dT} \right)_{T=T_n} \frac{dM}{dT}; \quad (2)$$

where  $\Theta(x)$  is the Heaviside step function. The parameter  $R$  measures the positive slope of the  $M(T)$  curve during zero-field heating. We have calculated  $R$  using a Gaussian size distribution centered at  $V = V_0$  and with width  $s$ . Our results for  $R$  are shown in Fig.2(d) for a particular choice of  $V_0$  as a function of  $s$ . We observe that  $R$  increases with the width of the distribution and saturates quickly. In this regime,  $R$  is almost independent of  $V_0$  and accordingly, the detailed nature of the distribution. We conclude that the memory effects will be best seen in samples with a dilute dispersion of particles but a very wide (flat) distribution of sizes. Indeed in this limit the relaxation is known [12] to be prominently dominated by magnetic viscosity characterized by a logarithmic relaxation in time. Not surprisingly, a logarithmic relaxation has been observed in the experiments of Sun et. al.[13] although the interpretation offered is different from ours. In order to substantiate our interpretation of the  $M$  vs.  $T$  data we have carried out hysteresis measurements and thereby coercivity estimation for both the interacting sample A and non-interacting sample B. The room-temperature DC magnetizations versus the applied magnetic field for both samples are shown in Fig.3. Clearly, for sample B the relaxation times are shorter than the measurement time, at 300K. Thus, there is no hystere-

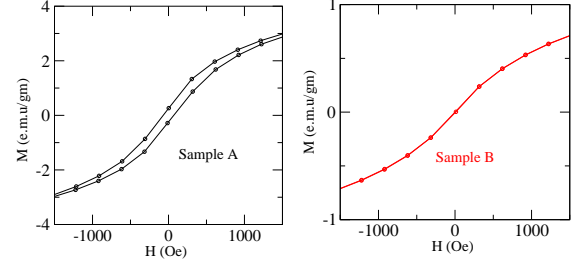


FIG. 3: (color on-line) Room temperature  $M-H$  curve of samples A and B. The hysteretic response of sample A points to the presence of strong dipolar interactions.

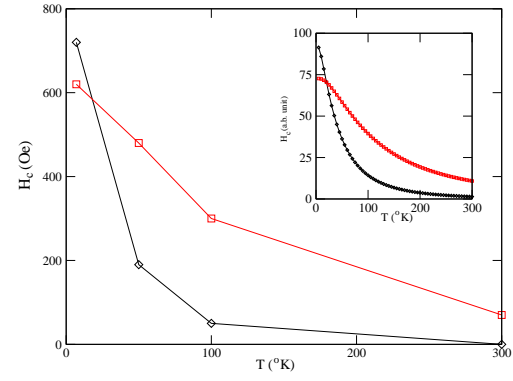


FIG. 4: (color on-line) Coercivity ( $H_c$ ) as a function of temperature for the interacting (2) and non-interacting (3) samples. The corresponding curves ( $H_c$  in arbitrary unit) obtained from our theory assuming a double delta function particle size distribution is shown in the inset.

sis loop and the coercivity (measured by the width along the abscissa on the zero-magnetization line) is also zero. On the other hand, for sample A, we observe a non-zero coercivity even at 300K due to the slowing down of relaxation because of the presence of an additional term proportional to  $V^2$  in the exponent of  $\langle V \rangle$  as mentioned above.

Next we repeat the above measurements down to 4K, using a SQUID magnetometer. The coercivity ( $H_c$ ) is plotted as a function of temperature ( $T$ ), in Fig.4. Because relaxation slows down for both sample A and sample B,  $H_c$  increases with decrease of  $T$  (Fig.4). The coercivity of the interacting sample A is larger than that non-interacting sample B for temperatures greater than 25K. However, at  $T = 25\text{K}$  a surprising crossover is detected,

where the coercivity for sample B shoots above that for sample A. We suggest that the reason for this behavior is that the term  $H$  in the exponent of  $(V)$  is replaced by  $H + H_c$ , where the mean field  $H_c$  arises from interaction:

$$H = V^2 \tanh\left(\frac{V(H + H_c)}{K_B T}\right) \quad (3)$$

where  $\alpha$  is a parameter that depends on the mean separation between the particles. The tanh term augments the  $V^2$  term below 25K, making the larger particles relax so slowly that they don't respond to  $H$  at all. Therefore, the larger particles are 'frozen out' from further consideration, making the mean relaxation time in the interacting case even smaller than that for the non-interacting case. This somewhat nonintuitive conclusion is further confirmed by our simulated coercivity computation, shown in Fig.4 (inset).

To verify our argument further we perform a separate set of experiments on both samples A and B as follows. We field-cool the samples down to 10K from 300K in the presence of  $H = 100$  Oe. At 10K the magnetic field is switched off and the relaxation of the magnetization measured. We find that the average relaxation time obtained by forcing an exponential fit to our data of sample A is 100 min and that of sample B is 25 min. We then heat the samples to 300K, and cool it back down to 10K at zero magnetic field. At 10K we switch on the magnetic field and wait for 2h. The magnetic field is then switched off and the magnetization measured. The relaxation time of sample B remains 25 min. but the relaxation time of sample A decreases to 30 min. This result is consistent with the reasoning described in the above paragraph. Therefore, for the low-temperature interacting system, larger particles are rendered magnetically inactive.

In conclusion, the strong history dependent effects seen in magnetization and coercivity measurements in  $\text{NiFe}_2\text{O}_4$  magnetic nanoparticles are interpreted as being due to arrested Neel relaxation. Our model is dramatically simplified by choosing just two volumes of the particles, on either side of the 'blocking' limit. Further corroboration of the proposed mechanism is achieved by performing measurements on an interacting system. Our results suggest that either by tuning the interaction (through changing inter-particle distance) or by tailoring the particle size distribution, these nanosized magnetic systems can be put to important application in memory devices. In particular, a flat volume distribution can be of great utility than a monodispersed distribution with a single

sharp peak.

SC thanks Kalyan Mandal for guidance on sample preparation. We acknowledge support from the Department of Science and Technology through its "Nanoscience Initiatives". SS acknowledges financial support from DST grant no: SP/S2/M-20/2001

- 
- [1] A.N. Goldstein, *Handbook of Nanophase Materials* (New York: Marcel Dekker Inc.) (1997).
  - [2] *Magnetic Properties of Fine Particles*, edited by J.L. Dormann and D. Fiorani (North-Holland, Amsterdam, 1992).
  - [3] K.M. Jinnuh and C.L. Chein, *Nanomaterials: Synthesis, Properties and Applications*, eds., A.S. Edelstein, R.C. Cammarata (Bristol: Institute of Physics).
  - [4] I.S. Jacobs and C.P. Bean, in *Magnetism III* (eds.) G.T. Rado and H. Suhl (New York: Academic) (1963).
  - [5] *Physical Principles of Magnetism*, A.H. Morrish, John Wiley New York, 1965.
  - [6] J. Frankel and J. Dorfman, *Nature* (London) 126, 274 (1930).
  - [7] C. Kittel, *Phys. Rev.* 70, 965 (1946).
  - [8] C.P. Bean and J.D. Livingston, *J. Appl. Phys.* 30, 120S (1959).
  - [9] Steen Mørup, Elisabeth Tronc, *Phys. Rev. Lett.* 72, 3278 (1994).
  - [10] L. Neel, *Ann. Geophys.* 5, 99 (1949); *Adv. Phys.* 4, 191 (1955).
  - [11] E.P. Wohlfarth, *J. Phys. F* 10, L241 (1980).
  - [12] R. Street and J.C. Woolley, *Proc. Phys. Soc. London, Sec. A* 62, 562 (1949). Also reviewed in S.D. Attagupta, *Relaxation Phenomena in Condensed Matter Physics*, Chapter XV, Academic Press, Orlando (1987).
  - [13] Y. Sun, M.B. Salamon, K. Gamier and R.S. Averback, *Phys. Rev. Lett.* 91, 167206 (2003).
  - [14] M. Sasaki, P.E. Jonsson, H. Takayama and P. Nordblad, *arXiv cond-mat/0311264 v2*.
  - [15] J.D. Wright and J.M. Sommersdijk, *Sol-Gel Materials, Chemistry and Applications* (London: Taylor and Francis) (2001).
  - [16] B.D. Cullity, *Elements of X-ray Diffraction* (1978).
  - [17] A.P. Young, *Spin Glasses and Random Fields*, eds., World Scientific, Singapore (1987).
  - [18] K.H. Fischer and J.A. Hertz, *Spin Glasses*, Cambridge University Press (1991).
  - [19] See for instance, K. Binder and W. Kinzel in *Heidelberg Colloquium on Spin Glasses* (J.L. Van Hemmen and I.M. Morgenstern), eds., Springer-Verlag, Berlin and New York, p.279 and references therein.
  - [20] S. Chakraverty, S. Chatterjee, S.D. Attagupta, A. Frydman, (Submitted)